

Bayesian evidence: can we beat MultiNest using traditional MCMC methods?

Rutger van Haasteren^{1*}

¹*Leiden University, Leiden Observatory, P.O. Box 9513, NL-2300 RA Leiden, the Netherlands*

printed 18 June 2018

ABSTRACT

Markov Chain Monte Carlo (MCMC) methods have revolutionised Bayesian data analysis over the years by making the direct computation of posterior probability densities feasible on modern workstations. However, the calculation of the prior predictive, the Bayesian evidence, has proved to be notoriously difficult with standard techniques. In this work a method is presented that lets one calculate the Bayesian evidence using nothing but the results from standard MCMC algorithms, like Metropolis-Hastings. This new method is compared to other methods like MultiNest, and greatly outperforms the latter in several cases. One of the toy problems considered in this work is the analysis of mock pulsar timing data, as encountered in pulsar timing array projects. This method is expected to be useful as well in other problems in astrophysics, cosmology and particle physics.

Key words: mathematics – methods: data analysis – statistics

1 INTRODUCTION

Bayesian inference has proved over the years to be a very powerful tool in many branches of science as it gives a very clear prescription of how to analyse datasets without loss of information, even for very complicated models. On the practical side, in performing Bayesian analysis two difficult problems often emerge:

1. Producing the posterior probability density functions (PDFs) for several interesting parameters requires marginalisation, i.e. the integration of the full joint posterior PDF over most model parameters. In a majority of cases this must be done numerically, and it is common to employ a Markov Chain Monte-Carlo (MCMC) algorithm for performing the integration.

2. Model selection requires the calculation of the Bayes factor: the ratio of the prior predictive values of two competing models. This prior predictive, or Bayesian evidence as we will call it, is the integral of the full joint posterior PDF over all model parameters. The calculation of this value can be notoriously difficult using standard techniques.

The use of Markov Chain Monte Carlo (MCMC) algorithms, such as the Metropolis-Hastings algorithm, has become extremely popular in the calculation of the marginal posterior PDFs. MCMC algorithms allow one to sample from posterior distribution of complicated statistical models, greatly reducing the effort involved in evaluating high dimensional numerical integrals. The problem with standard

MCMC algorithms lies in the fact that the normalisation constant of the marginal posterior PDFs is lost in the calculation, making it difficult to calculate the second of the above mentioned quantities.

Over the years, several methods capable of calculating the Bayesian evidence have been developed, such as using the harmonic mean (Newton & Raftery 1994) and parallel tempering (Earl & Deem 2005). The problems with these methods are the inaccuracy of the method for the harmonic mean, and the high computational cost for parallel tempering: this method can easily be 100 times more time-consuming than regular MCMC algorithms (Newman & Barkema 1999). More recent efforts include the Nested sampling algorithm (Skilling 2004), a greatly improved version of which has been implemented in MultiNest (Feroz et al. 2009, hereafter FHB09). These recent methods rely on a transformation of the integral to a 1-dimensional problem, and then use a clever trick for avoiding the calculation of the inverse of the cumulative posterior PDF. The MultiNest algorithm of FHB09 has been successfully tested on several (toy) problems, and seems to be much more efficient than traditional methods. However, since the MultiNest algorithm by design samples from the prior - not from the posterior - we believe that the MultiNest algorithm suffers more from the curse of dimensionality than the traditional MCMC algorithms (Evans 2006). When analysing complicated models with many parameters (~ 100 or more), the scaling with dimensionality is crucial.

In this paper we present a method to calculate the Bayesian evidence from the MCMC chains of regular MCMC

* Email: haasteren@strw.leidenuniv.nl

algorithms. This method can be applied to chains that have already been run, provided that the posterior values, calculated with normalised prior and normalised likelihood, have been saved together with the values of the parameters at each point in the chain. For several cases, the accuracy of the new method is significantly greater than that of other methods with the same amount of sampled points, provided that the MCMC has been properly run. The error on the Bayesian evidence can be reliably calculated using a bootstrap procedure.

The outline of the paper is as follows. In section 2 we briefly review the basic aspects of Bayesian inference for parameter estimation and model selection. Then we provide the reader with some necessary details on MCMC in section 3, where we also outline the new algorithm to calculate the Bayesian evidence. In section 4 we assess the strengths and weaknesses of the new method relative to those that use nested sampling or parallel tempering. In section 5 we test all competing algorithms on some toy problems like the analysis of pulsar timing data as encountered in pulsar timing array projects.

2 BAYESIAN INFERENCE

Bayesian inference methods provide a clear and consistent approach to parameter estimation and model selection. Consider a model, or Hypothesis, H with parameters $\vec{\Theta}$ for a dataset \vec{d} . Then Bayes' theorem states that

$$P(\vec{\Theta} | \vec{d}, H) = \frac{P(\vec{d} | \vec{\Theta}, H) P(\vec{\Theta} | H)}{P(\vec{d} | H)}, \quad (1)$$

where $P(\vec{\Theta}) := P(\vec{\Theta} | \vec{d}, H)$ is the posterior PDF of the parameters, $L(\vec{\Theta}) := P(\vec{d} | \vec{\Theta}, H)$ is the likelihood function, $\pi(\vec{\Theta}) := P(\vec{\Theta} | H)$ is the prior, and $z := P(\vec{d} | H)$ is the prior predictive or Bayesian evidence as we call it.

The Bayesian evidence is the factor required to normalise the posterior over $\vec{\Theta}$:

$$z = \int L(\vec{\Theta}) \pi(\vec{\Theta}) d^m \Theta, \quad (2)$$

where m is the dimensionality of $\vec{\Theta}$. This Bayesian evidence can then be used to calculate the so-called odds ratio in favor of model H_1 over H_0 , which allows one to perform model selection:

$$\frac{P(H_1 | \vec{d})}{P(H_0 | \vec{d})} = \frac{z_1 P(H_1)}{z_0 P(H_0)}, \quad (3)$$

where $P(H_0)$ and $P(H_1)$ are the prior probabilities for the different models. As with the prior for a model parameters, the prior probability for a model should be chosen to reflect the available information.

In traditional MCMC methods as used in parameter estimation problems, inferences are obtained by taking samples from a distribution that is proportional to the posterior PDF. Therefore one usually ignores the normalisation constant. This is acceptable since these methods lose the information about the normalisation anyway. But in contrast to parameter estimation problems, in model selection the

Bayesian evidence plays a central role: it is a measure for how well the data supports the model.

The average of the likelihood over the prior distribution, the evidence, is larger for a model if more of its parameter space is likely and smaller for a model with large areas in its parameter space having low likelihood values. Even if the likelihood function has high peaks, in order to increase the evidence these peaks must compensate for the areas in its parameter space where the likelihood is low. Thus the evidence automatically implements Occam's razor: a simpler theory with compact parameter space will have a larger evidence than a more complicated model, unless the latter is significantly better at explaining the data.

3 MARKOV CHAIN MONTE CARLO

Markov Chain Monte Carlo methods (MCMC) can be used to sample from very complicated, high dimensional distributions; for Bayesian inference it is the posterior, but it could be any distribution. The method presented in this paper could be useful for integration problems other than Bayesian evidence calculation, so we use the more general $f(\vec{\Theta})$ to denote this function. The samples drawn from this function can then be used to perform the integrals we need for the marginal posterior PDFs and, as we show, for the Bayesian evidence. The idea is quite straightforward: a large number of samples drawn from a distribution proportional to $f(\vec{\Theta})$ will end up being distributed with a sample density proportional to $f(\vec{\Theta})$. The exact mechanism that produces these samples can differ between MCMC methods and is irrelevant for the purposes of this paper, but the result is always a large number of samples distributed according to $f(\vec{\Theta})$. The main advantage of this is that we do not have to sample from the entire volume of the parameter space or the prior, but only from a small fraction of it: the fraction where the function has a high value. Especially for functions in high-dimensional parameter spaces this feature is crucial.

In section 3.1 we show that all information needed to calculate the Bayesian evidence is already present in the samples of the MCMC. Then we give a practical example of how to calculate the integral in practice in section 3.3.

3.1 Volume calculation

Consider the unnormalised distribution:

$$f(x, y) = \exp(-ax^2 - by^2), \quad (4)$$

where a and b are arbitrary model parameters. For the values $a = 1/5$ and $b = 2/5$, a Metropolis algorithm with $N = 40000$ samples yield a distribution of samples similar to Figure 1. We use the notation $\vec{\Theta}_i = (x_i, y_i)$ to indicate the i^{th} sample. We would now like to calculate the integral

$$I = \int \int f(x, y) dx dy. \quad (5)$$

In MCMC algorithms, it is usually required or straightforward to calculate the function values $f(\vec{\Theta}_i)$ for each sample, and these values are often stored together with the values of the parameters. These function values can be used to calculate the integral if we treat the MCMC samples in parameter space as an irregular grid. The most obvious and exact way

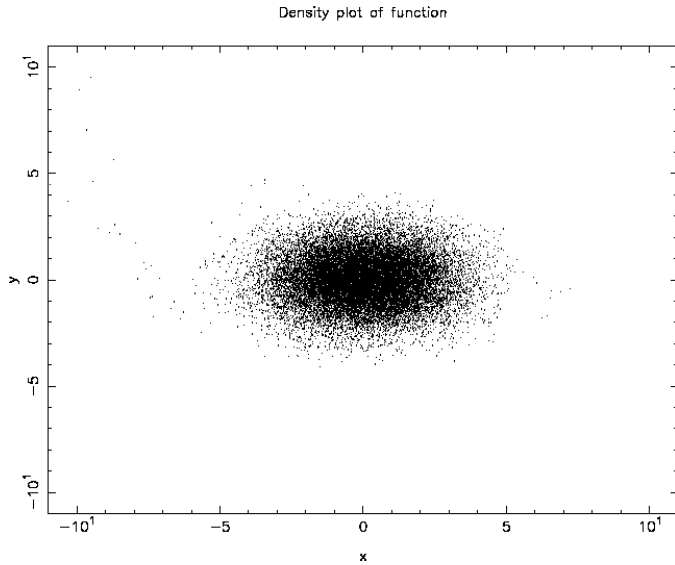


Figure 1. A scatter plot of 40000 samples, drawn using a Metropolis algorithm from the function $f(x, y) = \exp(-ax^2 - by^2)$, with $a = 1/5$ and $b = 2/5$. We have included the burn-in period in this plot, even though that part of the chain should be discarded for any further calculations.

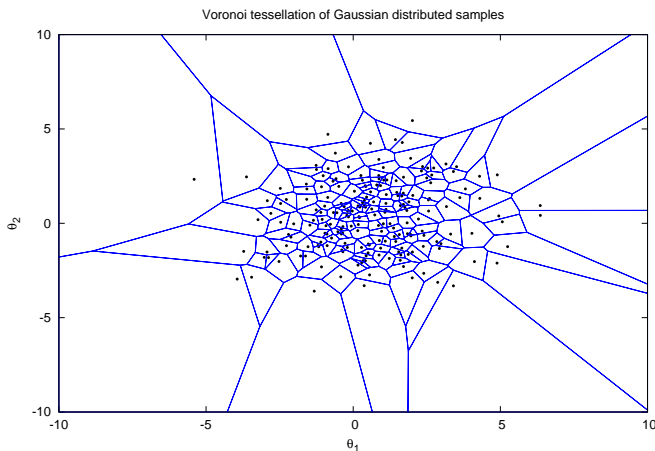


Figure 2. An example of a Voronoi tessellation. Here we have taken 200 samples from a 2-dimensional Gaussian distribution as the centres of the Voronoi diagram.

to do this is to calculate the Voronoi tessellation for the samples in the parameter space, an example of which is given in Figure 2. The samples are then the centres of the Voronoi cells, and the integral can be calculated as follows:

$$I \approx \sum_i f(\vec{\theta}_i) O_i, \quad (6)$$

where O_i is the area of the i^{th} Voronoi cell, and we only sum over closed cells (with finite area). Theoretically, this procedure converges to the correct value in all cases for large number of samples N . However, although Voronoi tessellations can be computed for any dimensionality, this becomes computationally prohibitive in practice for problems with high dimensionality (Edelsbrunner & Shah 1996). This pro-

cedure does illustrate that all information needed to evaluate the integral I is present in the MCMC chain.

3.2 Estimating the covered parameter volume

As we have shown in section 3.1, the integral I can be approximated by the summation over the function values $f(\vec{\theta}_i)$ times the Voronoi cell size O_i . The value O_i is the parameter volume occupied by the Voronoi cell of the i^{th} MCMC sample, so in the rest of this paper we call O_i the parameter volume of the i^{th} sample. Similarly, the parameter volume of the entire chain can now be approximated by:

$$O = \sum_{i=1}^N O_i, \quad (7)$$

where O is the parameter volume of the entire MCMC chain, and N is the number of samples in the chain.

We now show that we do not need the Voronoi tessellations to calculate the parameter volume and the integral. For the rest of this section we regard the more general case that we have an n -dimensional parameter space, instead of the 2-dimensional case of the above example. In any MCMC algorithm, the density of points of the chain at a certain point $\vec{\theta}_i$ in parameter space will become proportional to the function value $f(\vec{\theta}_i)$ for large N . Therefore,

$$\lim_{N \rightarrow \infty} O_i = \frac{\alpha}{f(\vec{\theta}_i)}, \quad (8)$$

where α is a proportionality constant to be determined. If we somehow can estimate the constant α for this chain, we can immediately calculate the integral by $I = N\alpha$.

The proportionality constant α can be estimated for a certain chain by regarding a small subset $F_t \subset \mathbb{R}^n$ of the parameter space for which:

1. we can calculate what the volume V_t of the small subset is.
2. the subset F_t is sufficiently and completely populated by MCMC samples: all parts of F_t should have a sample density proportional to $f(\vec{\theta})$

MCMC algorithms are employed in order to avoid having to draw samples from the entire parameter space, so we have to be careful to choose the right test subset in order to fulfill requirement 2. If we have found such a subset F_t , the following equation allows us to estimate α :

$$V_t = \sum_{\vec{\theta}_i \in F_t} \frac{\alpha}{f(\vec{\theta}_i)}. \quad (9)$$

The calculation of the integral is now trivial:

$$I = N\alpha. \quad (10)$$

3.3 A practical algorithm

In this section we construct a simple practical algorithm for numerically calculating integrals using regular MCMC methods. As stated in section 3.2, we need to define a small subset of the parameter space that is sufficiently populated by MCMC samples. The most obvious choice would be to look for a peak in the distribution. In the case of multimodal posteriors, we should take samples that 'belong'

to one specific mode. Clustering algorithms like X-means (Pelleg & Moore 2000), and G-means (Hamerly & Elkan 2003) can be used for this.

Assuming that we have found M samples that belong to a specific mode, we can then define a subset F_t as follows. Assume that the M samples are sorted according to their function value $f(\vec{\Theta}_i)$, with $f(\vec{\Theta}_0)$ the highest value. We then first approximate the maximum of $f(\vec{\Theta})$ as:

$$\vec{\mu} = \frac{1}{k} \sum_{i=1}^k \vec{\Theta}_i, \quad (11)$$

where $k = aM$ is a small fraction of M , dependent on the shape of the mode. We use $a = 1/20$ in several cases. We now define our subset F as an ellipsoid with centre $\vec{\mu}$, and covariance matrix C , defined by:

$$C = \frac{1}{n} \sum_{i=1}^n (\vec{\Theta}_i - \vec{\mu}) (\vec{\Theta}_i - \vec{\mu})^T, \quad (12)$$

where $n = bM$ is a fraction of M , again dependent on the shape of the mode. We use $b = 1/5$ in several cases. All samples within this ellipsoid of size $\sqrt{r^2 \det C}$ satisfy:

$$(\vec{\Theta} - \vec{\mu})^T C^{-1} (\vec{\Theta} - \vec{\mu}) \leq r^2. \quad (13)$$

We adjust the parameter r^2 such that $l = cM$ samples satisfy this relation. It is crucial that we choose l to be as large as possible, while still satisfying the requirement that the entire ellipsoid is sufficiently populated with samples. If l is too small, we will not achieve very high accuracy for our integral I , but if l is too large, we have underpopulated parts of the ellipsoid which results in the wrong outcome. We use $c = 1/3$ in several cases.

We now have all the ingredients needed to calculate the integral I , as the Volume of our k -dimensional subset is given by:

$$V_t = \frac{r^k \pi^{\frac{k}{2}}}{\Gamma(1 + \frac{k}{2})} \sqrt{\det C}. \quad (14)$$

This, combined with equations (9) and (10) allows us to evaluate the integral.

We would like to note that this prescription is merely one of many that could be used. In this case we have defined our subset F_t as an ellipsoid located at a maximum of our integrand, but any other subset that meets the criteria of section 3.2 will suffice.

3.4 Error estimates

A MCMC algorithm generates samples according to the distribution $f(\vec{\Theta})$. Consider the amount of samples inside the subset F_t . This amount follows a Poissonian distribution with mean and variance equal to cM . We thus obtain the theoretical estimate for the error in the integral:

$$\Delta I = \frac{1}{\sqrt{cM}} I. \quad (15)$$

As we show in section 5.1, this estimate is reliable for Monte Carlo algorithms that yield uncorrelated samples. In practice, however, many MCMC algorithms produce correlated samples since a whole chain of samples is used

(Roberts et al. 1997). As we show in section 5, the use of correlated MCMC samples for numerical integral as proposed in this paper invalidates the error estimate of equation (15).

Having efficiency as one of our goals, we would like to produce reliable error-bars on our numerical integral using the correlated MCMC samples. We propose to use a bootstrap method (Efron 1979). In the case of several chains, one can use the spread in the estimates based on different chains to estimate the error of the integral. In the case of a single chain, we propose to divide the chain in 10 succeeding parts, and use the spread of the integral in those 10 parts to estimate the error of the numerical integral. In section 5.4 we test the error estimates discussed here extensively.

4 COMPARISON TO OTHER METHODS

Although the formalism developed in this paper is quite generally applicable, in practice there are caveats for each integration problem that one needs to be aware of in order to choose the right integration algorithm. In this section we discuss the strengths and the weaknesses of the method developed in this paper, and we compare it to Nested sampling, and Parallel tempering.

For all algorithms, the main criteria that we cover are efficiency, accuracy and robustness.

4.1 Method using traditional MCMC

The main problem that MCMC algorithms try to tackle is that of parameter space reduction; the full parameter space over which we would like to evaluate the integral is too large, which is why we cannot use a regular grid. The idea behind MCMC algorithms is that of *importance sampling*: only draw samples in the regions of parameter space where the function value $f(\vec{\Theta})$ is high enough to significantly contribute to the integral. This can be done by drawing samples from a distribution $P(\vec{\Theta})$ that resembles the function $f(\vec{\Theta})$, with the optimal choice being $P(\vec{\Theta}) = f(\vec{\Theta})$. MCMC are specifically designed to satisfy this optimal relation, making MCMC methods optimally efficient from a theoretical point of view (Roberts et al. 1997). In Figure 1 we show an example of samples generated with a Metropolis MCMC algorithm, released on a 2-dimensional Gaussian function.

The drawback of MCMC algorithms is that due to the parameter space reduction one can never be sure that all important parts of the parameter space have been covered. Some functions have many distinct peaks, the so-called modes of the function. MCMC algorithms often have difficulty to make the chain move from one mode to another. If the function $f(\vec{\Theta})$ is highly multimodal, we must make sure that the sample density ratio between the modes is right and that we have reached all the important modes in the entire parameter space.

An additional practical challenge with the method developed in this paper is to make sure that we have constructed a subset of the parameter space that is sufficiently populated with samples. In the case of a not very peaked, or highly degenerate function this requires special care.

4.2 Nested sampling

The nested sampling algorithm is a Monte Carlo technique aimed at accurate evaluation of numerical integrals, while staying efficient (Skilling 2004). The algorithm solves the problems of regular MCMC algorithms by starting with sampling from the original parameter space. In the case of Bayesian evidence calculation this is equivalent to sampling from the prior distribution of the parameters. The density with which the parameter space is sampled is adjustable in the form of an amount n_L of so-called live points; the number of points evenly distributed among the part of the parameter space we are exploring. At the start of the algorithm, the live points are evenly distributed over the entire parameter space. Then parameter space reduction is achieved by replacing the live points one-by-one under the restriction that the newly sampled live points are higher than the lowest one we have not replaced yet. Effectively this is the same as shrinking the parameter space by a fixed factor every time we replace a new live point, ultimately sampling only the part of the function close to the maximum.

A big advantage of the nested sampling algorithm is that one generates samples directly from the whole parameter space. If n_L is chosen high enough, i.e. there is a high enough sampling density in the parameter space, there is a very low probability that a mode of the distribution $f(\vec{\Theta})$ will be missed. This is one of the difficulties in many MCMC implementations.

A big disadvantage of the nested sampling algorithm is that one directly generates samples from the whole parameter space, instead of from a distribution that more closely resembles the function $f(\vec{\Theta})$ we want to integrate. This method will therefore never reach the efficiency that traditional MCMC methods offer. In Figure 3 we show an example of samples generated with a nested sampling algorithm, applied to a 2-dimensional Gaussian function. In higher dimensional problems, as discussed in section 5.1, the direct sampling from the whole parameter space can lead to serious efficiency problems that need to be solved.

4.3 Parallel tempering

Parallel tempering (PT) is an algorithm spawned from the desire to solve the problems of traditional MCMC methods. PT algorithms possess better mixing properties, allowing the chain to “escape” local extrema, and allow one to calculate the complete integral, or in our case the Bayesian evidence (Earl & Deem 2005). Let us briefly review PT in this section, without discussing it in too much detail.

The main idea of PT is that of parameter space exploration by adding an imaginary inverse temperature β to the system, changing the integrand of our integral to:

$$f_\beta(\vec{\Theta}) = \left(f(\vec{\Theta})\right)^\beta. \quad (16)$$

Then many MCMC chains are released in the parameter space, each with a different temperature $\beta \in [0, 1]$. A clever swapping system is employed, allowing the chain with $\beta = 1$ - the “true” chain - to swap parameters with chains of higher temperature every now and then provided that such a high-temperature chain was able to reach a point in parameter space with high $f(\vec{\Theta})$. This trick allows the coldest system, the “true” chain with $\beta = 1$, to escape local extrema.

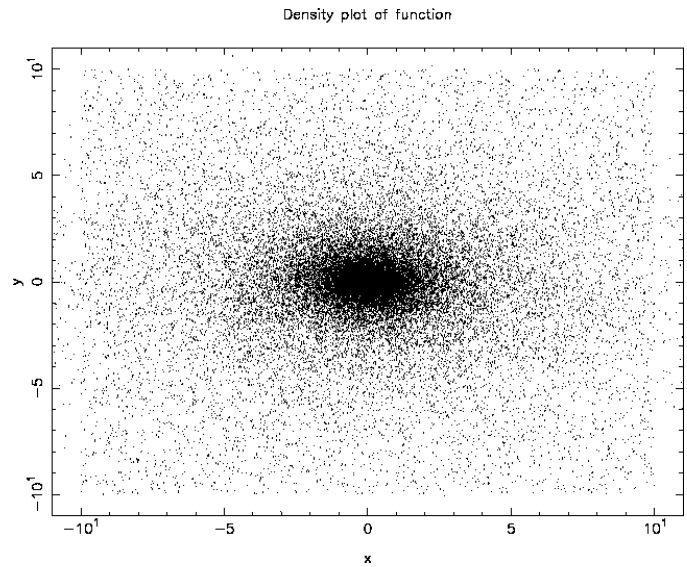


Figure 3. A scatter plot of 40000 samples, drawn using a nested sampling algorithm with 5000 live points from the function $f(x, y) = \exp(-ax^2 - by^2)$, with $a = 1/5$ and $b = 2/5$.

The integral over $f(\vec{\Theta})$ is calculated by using all chains, not just the one with $\beta = 1$, as follows. We first define a partition function:

$$Z(\beta) = \int d\vec{\Theta} f_\beta(\vec{\Theta}), \quad (17)$$

which has a logarithmic derivative of:

$$\frac{d}{d\beta} \log(Z(\beta)) = \frac{1}{Z(\beta)} \frac{d}{d\beta} Z(\beta) = \left\langle \log\left(f(\vec{\Theta})\right) \right\rangle_\beta, \quad (18)$$

where $\langle \cdot \rangle_\beta$ is the expectation value of a quantity over a distribution proportional to $f_\beta(\vec{\Theta})$. Since we know that our desired integral can be expressed as $I = Z(1)$, equation (18) is all we need to calculate it:

$$\log(Z(1)) = \log(Z(0)) + \int_0^1 d\beta \left\langle \log\left(f(\vec{\Theta})\right) \right\rangle_\beta. \quad (19)$$

The observant reader will have noted that we have neglected to mention the size $Z(0)$ of the parameter space that we explore with our chains. The high temperature chain with $\beta = 0$ is unbounded by the function $f(\vec{\Theta})$, and therefore will transverse the entire parameter space. We should make sure that we limit the size of the parameter space as much as possible, without missing any peaks of $f(\vec{\Theta})$.

The main advantages of Parallel tempering are that it explores the entire parameter space, even in the presence of strong local peaks, and that the Bayesian evidence can be calculated. These advantages are accompanied with the large computational costs of the extra chains with $\beta \neq 1$, which has resulted in the need for alternative methods like MultiNest. As MultiNest is supposed to outperform PT in virtually all cases (FHB09), we will compare our method to MultiNest only in section 5.

5 APPLICATIONS AND TESTS

In this section we consider several toy models, and we apply several integration algorithms to these toy models as to compare the algorithms. In this whole section we have two ways

to use the MCMC algorithm. To produce correlated samples, we use a regular Metropolis-Hastings algorithm where we use the entire chain. To produce uncorrelated samples, we use the same algorithm, but we only store one in every j samples produced by the algorithm. This does require us then to run the chain j times longer to produce the same number of samples. We choose j high enough that there is negligible correlation between 2 succeeding used samples; in the case of a n -dimensional Gaussian as in section 5.1 we use $j = 100$.

5.1 Toy model 1: a high-dimensional Gaussian

We first consider a problem that is a typical example of what MCMC algorithms were designed for: a highly peaked, high-dimensional function. The curse of dimensionality prohibits any direct numerical integration scheme on a fine grid, but analytical integration is possible. Consider the multiplication of n Gaussian functions,

$$f_1(\vec{x}) = \prod_{i=1}^n \sqrt{\frac{a_i}{2\pi}} \exp\left(-\frac{1}{2}a_i x_i^2\right), \quad (20)$$

with a_i the width of the Gaussian in the i^{th} direction. Now let us perform a volume preserving coordinate transformation using a random orthogonal matrix R as follows: $\vec{\Theta} = R\vec{x}$. If we introduce a matrix $A_{ii}^{-1} = a_i = 1 + i$ with $A_{ij}^{-1} = 0$ for $i \neq j$, we then have a highly degenerate high-dimensional Gaussian function:

$$f_1(\vec{\Theta}) = \frac{1}{(2\pi)^{n/2} \sqrt{\det C}} \exp\left(-\frac{1}{2}\vec{\Theta}^T C^{-1} \vec{\Theta}\right), \quad (21)$$

where we have introduced the coherence matrix $C = RAR^T$.

We now apply in turn the MultiNest algorithm and the algorithm developed in this paper combined with Metropolis-Hastings to the multi-dimensional Gaussian for various number of dimensions.

For the MultiNest algorithm, we use a number of live points $L = 50n$ with n the number of dimensions, and we have set the sampling efficiency to $e = 0.3$ and the evidence tolerance to $t = 0.1$ as advocated in FHB09¹.

We set up the Metropolis-Hastings algorithm to have an acceptance ratio equal to the optimal value of 23.4% (Roberts et al. 1997). The parameters of the algorithm advocated in section 3.3 have been set to: $a = 1/20, b = 1/5, c = 1/3$. We have used the number of samples N used by the MultiNest algorithm as the number of samples in our MCMC chain. However, we realise that the MultiNest algorithm might be improved in the future, as the algorithm is still under construction. The lowest efficiency (used samples / drawn samples) we encountered for this toy-problem was $e = 0.08$; we therefore estimate that the error-bars could be decreased with a factor of maximally $\sqrt{1/0.08} \approx 3.5$. The results of this toy-model are shown in table 1.

¹ We have not used wrapping for the parameters. Wrapping does speed up the sampling, but somehow the resulting evidence estimates are less accurate

log(I) for different algorithms				
n	# N	MultiNest	Unc. MCMC	Cor. MCMC
2	2902	-0.17 ± 0.18	-0.018 ± 0.025	0.03 ± 0.025
4	7359	0.20 ± 0.17	0.007 ± 0.024	-0.01 ± 0.03
8	24540	0.17 ± 0.17	-0.01 ± 0.01	0.02 ± 0.03
16	10^5	0.05 ± 0.18	0.001 ± 0.006	0.004 ± 0.03
32	10^6	1.43 ± 0.17	0.004 ± 0.004	-0.015 ± 0.010
64	4.10^6		-0.0004 ± 0.0007	-0.02 ± 0.016
128	10^7		0.0006 ± 0.0004	-0.05 ± 0.03

Table 1. The log-integral values of the function f_1 of equation (21). N is the number of samples, and n is the number of dimensions. The analytically integrated value is $\log I = 0$ for all values of n . For $n \geq 64$, we were not able to successfully complete the MultiNest algorithm with said parameters due to limited computational power. Memory size was the limiting factor for the regular MCMC.

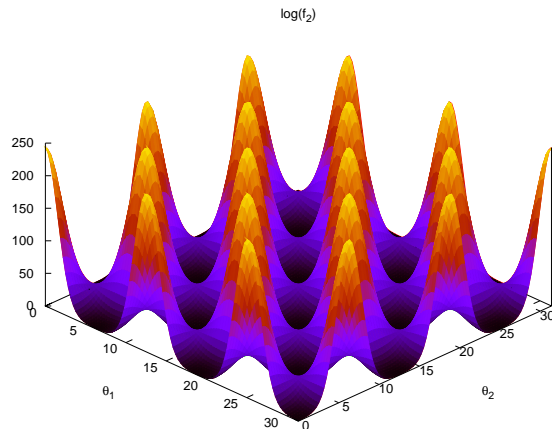


Figure 4. Toy-model 2: the eggbox of equation (22)

5.2 Toy model 2: egg-box function

Just as in FHB09, we now consider a highly multimodal two-dimensional problem for which the function resembles an egg-box. The function is defined as:

$$f_2(\vec{\Theta}) = \exp[2 + \cos(\Theta_1) \cos(\Theta_2)]^5, \quad (22)$$

where we set the domain of the function equal to $[0, 10\pi]$ for both parameters. The shape of this function is shown in Figure 4. This is a typical problem where difficulties arise for traditional MCMC algorithms. Many solutions have been proposed for situations like this (Newman & Barkema 1999), but in practice one needs to have additional information about the problem for any of those solutions to be reliable. For the sake of clarity of this paper, we do not concern us with the practical implementation of the MCMC algorithm. We assume that a suitable trick can be found for the problem at hand so that the algorithm proposed in this paper can be used. For the eggbox toy-model we will use a jump-technique. At each iteration of the MCMC algorithm, there is a small probability, 1% in this case, that the chain will jump to a random neighbouring mode.

The MultiNest algorithm is ideally suited for this problem, as this is a low-dimensional multimodal function. With

log(I) for different algorithms

# N	MultiNest	Unc. MCMC	Cor. MCMC
60210	240.19 ± 0.05	240.19 ± 0.027	240.23 ± 0.05

Table 2. The log-integral values of a single mode of the eggbox function of equation (22) The fine-grid integrated value is $\log I = 240.224$

enough live samples all modes should be easily discovered, and the peaks are symmetric and well-behaved. We run MultiNest on this problem with the same parameters as in FHB09: We use $L = 2000$ live points, efficiency $e = 0.3$, and tolerance $t = 0.1$.

Table 2 shows the results of this analysis². For evaluating the integral with the MCMC chain, we have taken a total of $N = 60210$ samples as was done with MultiNest, but we have used only the samples of one single peak in equation (9). The amount of samples in a single peak is $2/25$ of the total amount of samples, leading to loss of accuracy. Though more sophisticated methods can be constructed by, say, averaging the values of the proportionality constant α of equation (8) for all individual peaks, we show here that we only need to find one single portion of the parameter space that is sufficiently populated to calculate a reliable value for the integral.

5.3 Application in Pulsar Timing

In pulsar timing data analysis, one often encounters datasets of which the exact statistics are not well known. Bayesian model selection would provide the ideal tool to obtain information about the power spectra present in the data. van Haasteren et al. (2009, hereafter vHMLL) give a full description of the Bayesian data analysis for pulsar timing arrays, but their work lacks a method to calculate the Bayesian evidence from the MCMC samples. In this section, we use a pulsar timing mock dataset to show that the method developed in this paper is well-suited for Bayesian evidence calculation in pulsar timing problems. We also use MultiNest to analyse this dataset, and we compare the two results.

For the purposes of this paper, the description of the pulsar timing posterior distribution is kept brief; full details can be found in vHMLL. The data of pulsar timing experiments consists of the arrival times of pulsar pulses (TOAs), which arrive at the earth at highly predictable moments in time (Hobbs et al. 2006). The deviations from the theoretically predicted values of these TOAs are called the timing-residuals (TRs). These TRs are the data we concern ourselves with in this example.

Consider $n = 100$ TRs, denoted as $\vec{\delta t}$, observed with intervals between succeeding observations of 5 weeks. Assume that we are observing a stable and precise millisecond pulsar with timing accuracy about $\sigma = 100$ ns (the error bars on the TRs). Usually σ not precisely known, since pulsar timers generally assume that their estimate of the error bar is slightly off. Several datasets of millisecond pulsars also seem

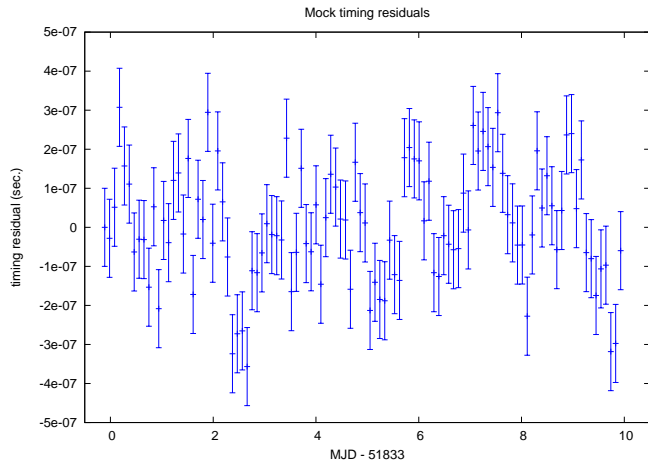


Figure 5. The mock timing-residuals we have analysed with both MultiNest and the method developed in this paper

to contain correlated low frequency noise (Verbiest et al. 2009). We therefore also allow for some correlated timing-noise in the data, with a power-spectrum given by:

$$S(f) = r^2 \gamma \exp(-\gamma f), \quad (23)$$

where f is the frequency, r is the amplitude of the correlated timing-noise in ns, and γ is the typical size of the structures that appear in the data due to this correlated timing-noise. Following vHMLL, we can now write the likelihood function for the TRs as a multi-dimensional Gaussian:

$$P(\vec{\delta t} | \sigma, r, \gamma) = \frac{1}{\sqrt{(2\pi)^n \det C}} \exp\left(-\frac{1}{2} \vec{\delta t}^T C^{-1} \vec{\delta t}\right), \quad (24)$$

where C is an $(n \times x)$ matrix, with elements defined as:

$$C_{ij} = \sigma^2 \delta_{ij} + r^2 \frac{\gamma^2}{\gamma^2 + \tau_{ij}^2}, \quad (25)$$

with δ_{ij} the Kronecker delta, and τ_{ij} is the time difference between observation i and observation j .

Simulating a mock dataset from such a Gaussian distribution is quite straightforward; for details see vHMLL. We now analyse a mock dataset, shown in Figure 5, generated with parameters: $\sigma = 100$ ns, $r = 100$ ns, and $\gamma = 2$ yr. We assume uniform prior distributions for all parameters: $\sigma \in [0, 1000]$ ns, $r \in [0, 1000]$ ns, and $\gamma \in [0, 10]$ yr. The posterior is then sampled using both MultiNest and a Metropolis-Hastings algorithm, resulting in marginalised posterior distributions as shown in Figure 6 & 7. Bayesian evidence values are in good agreement between the two methods:

$$\begin{aligned} z_{\text{MCMC}} &= \exp(1523.12 \pm 0.17) \\ z_{\text{MultiNest}} &= \exp(1522.93 \pm 0.15). \end{aligned} \quad (26)$$

For both methods, the same number of samples has been used: $N = 9617$.

5.4 Precision tests

We now test the accuracy of the algorithm by running it many times on the same toy-problem, and then considering the statistics of the ensemble. We found the 16-dimensional Gaussian of section 5.1 to be an illustrative example. Just

² The true value is different from the one noted in FHB09. We have taken the hypercube transformation into account in our calculations.

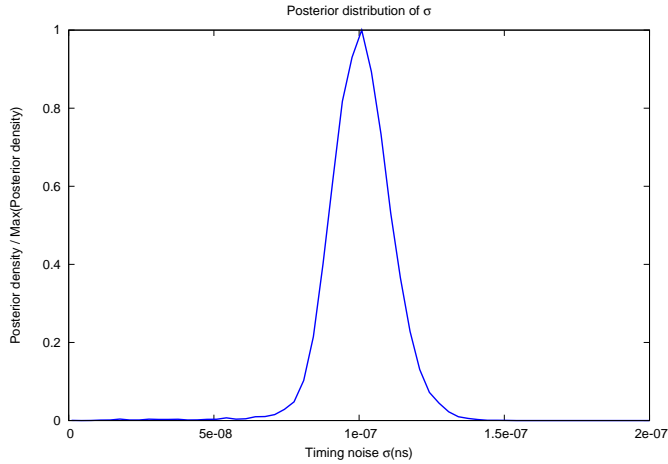


Figure 6. The marginalised posterior of the σ parameter, sampled using a Metropolis-Hastings MCMC method.

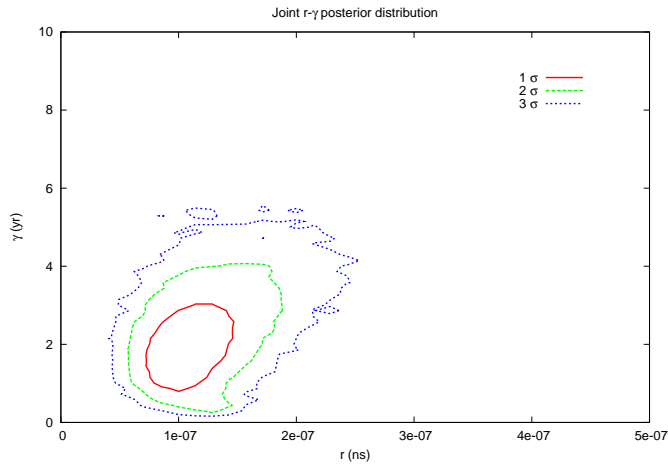


Figure 7. The marginalised posterior of the r and γ parameters, sampled using a Metropolis-Hastings MCMC method.

as in table 1, we take $N = 10^5$ and $c = 0.3$, and then we run $n = 10^4$ Metropolis-Hastings chains on this toy-problem. For the i^{th} chain we then calculate the integral I_i and bootstrap error estimate σ_i^{BS} . We have presented the results of this analysis as a histogram of I_i values in Figure 8. Several useful quantities that characterise the ensemble are:

$$\begin{aligned} \bar{I} &= \frac{1}{n} \sum_{i=1}^n I_i = 0.980 \\ \bar{\sigma} &= \sqrt{\frac{1}{n} \sum_{i=1}^n (I_i - \bar{I})^2} = 0.028 \\ \bar{\sigma}^{\text{BS}} &= \sqrt{\frac{1}{n} \sum_{i=1}^n (\sigma_i^{\text{BS}})^2} = 0.027, \end{aligned} \quad (27)$$

where \bar{I} is the integral average, $\bar{\sigma}$ is the rms of the integral values, and $\bar{\sigma}^{\text{BS}}$ is the rms value of the bootstrap errors.

Figure 8 shows that the bootstrap error estimate is quite correct, since $\bar{\sigma} \approx \bar{\sigma}^{\text{BS}}$. However, though smaller than $\bar{\sigma}$, there is a significant deviation in the value of \bar{I} compared

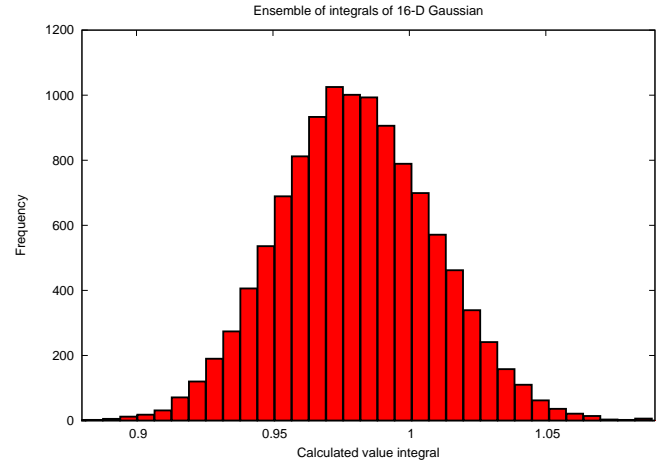


Figure 8. Histogram of the frequency of calculated integral using the method developed in this paper. We have taken the 16-dimensional Gaussian of equation (21) as integrand. Here we have analysed it with $N = 10^5$, and $c = 0.3$. This histogram has mean and standard deviation: $\bar{I} = 0.980$, $\bar{\sigma} = 0.028$. The rms of the bootstrap error of the ensemble was $\bar{\sigma}^{\text{BS}} = 0.027$

to the true value $I = 1$. As we have discussed in section 3.2, the criterion for the algorithm to converge to the correct value is that the small subset F_t is sufficiently populated by MCMC samples with density proportional to $f(\bar{\Theta})^{-1}$.

In order to test whether the deviation of \bar{I} from the true value $I = 1$ is due to not fulfilling requirement 2 of section 3.2, we will perform 3 additional tests. In all 3 cases, we will construct a new ensemble of MCMC chains identical to the ensemble above, except for one parameter. The differences with the above mentioned ensemble are:

1. Instead of a correlated MCMC chain, we use an MCMC chain of uncorrelated samples, produced by performing a regular MCMC but only storing every 100th sample.
2. $N = 10^7$, instead of $N = 10^5$. This results in much more samples in the subset F_t .
3. $c = 0.7$, instead of $c = 0.3$, which also results in more samples in the subset F_t .

We present the results of this analysis as the values of equation (27) in table 3. All adjustments seem to improve the precision of the algorithm. Several notes are in order:

1. The only reason we can increase c is because we know exactly what the integrand looks like. In practical applications this is probably not an option. Also note that bootstrap error increases, indicating that estimate of the integral is less stable.
2. The fact that the uncorrelated chain performs as well as theoretically possible according equation (15) shows that the algorithm suffers significantly under the use of correlated MCMC chains.
3. Increasing the amount of samples in a chain makes the calculated integral more reliable, as the subset F_t is more densely populated. Note that this large chain is build up of small chains that would yield a biased value.

Ensemble statistics for different parameters					
Cor./Unc.	N	c	\bar{I}	$\bar{\sigma}$	$\bar{\sigma}^{\text{BS}}$
Cor.	10^5	0.3	0.980	0.028	0.027
Unc.	10^5	0.3	1.000	0.006	0.006
Cor.	10^7	0.3	1.000	0.003	0.003
Cor.	10^5	0.7	0.994	0.020	0.034

Table 3. The statistics of equation (27) for various ensembles of $n = 10^4$ MCMC runs on a 16-dimensional Gaussian. The first chain has the same parameters as used in section 5.1. The other chains differ in either number of samples per chain N , the size c of the subset F_t , or whether or not the samples in a chain are correlated. Note that the error in the uncorrelated chain equals the theoretical Poissonian limit of $\sigma = \sqrt{1/cN} = 0.006$.

6 DISCUSSION AND CONCLUSIONS

We develop and test a new algorithm that uses traditional MCMC methods to accurately evaluate numerical integrals that typically arise when evaluating the Bayesian evidence. The new method can be applied to MCMC chains that have already been run in the past so that no new samples have to be drawn from the integrand. We test the new algorithm on several toy-problems, and we compare the results to other algorithms: MultiNest and Parallel tempering. We conclude that there is no single algorithm that outperforms all others in all cases. High-dimensional, peaked problems are better tackled using a traditional MCMC method, whereas very complicated multimodal problems are probably best handled with MultiNest. When applicable, the new algorithm significantly outperforms other algorithms, provided that the MCMC has been properly executed. This new algorithm is therefore expected to be useful in astrophysics, cosmology and particle physics.

We have demonstrated that the new algorithm suffers under the use of correlated MCMC chains, produced by using the entire chain of a particular MCMC method like Metropolis-Hastings. If the new algorithm is used in combination with an uncorrelated chain, the accuracy of the numerical integral can reach the theoretical limit for stochastic methods: $\sigma = I/\sqrt{N}$, with σ the uncertainty, I the value of the integral, and N the amount of MCMC samples. Using correlated MCMC samples can significantly increase the integral uncertainty, and longer MCMC chains are needed for the integral to converge. Additional tests to assess convergence are required.

6.1 Comparison to other work

When this paper was already submitted to Monthly Notices, a preprint by Weinberg (2009) appeared on the arxiv which also attempts to construct an algorithm to calculate the Bayesian evidence using MCMC samples of the posterior. Weinberg first discusses the flaws of the harmonic mean estimator, and then proposes 2 algorithms to overcome these flaws. Weinberg then tests these interesting modifications to the harmonic mean estimator on simulated datasets. The algorithm proposed by Weinberg bears some resemblance to the algorithm in this paper in that one should only use a well-sampled subset of the parameter space when estimating the Bayesian evidence.

ACKNOWLEDGEMENTS

We would like to thank Yuri Levin, Christian Röver, Reinhard Prix, Gerard Barkema, and Chael Kruip for insightful discussions. This research is supported by the Netherlands organisation for Scientific Research (NWO) through VIDI grant 639.042.607.

REFERENCES

- Earl D. J., Deem M. W., 2005, *Physical Chemistry Chemical Physics (Incorporating Faraday Transactions)*, 7, 3910
- Edelsbrunner H., Shah N. R., 1996, *Algorithmica*, 15, 223
- Efron B., 1979, *Ann. of Stat.*, 7, 1
- Evans M. J., 2006, in J. M. Bernardo, M. J. Bayarri, J. O. Berger, A. P. Dawid, D. Heckerman, A. F. M. Smith, M. West ed., *Proceedings of the Eighth Valencia International Meeting Discussion of Nested Sampling for Bayesian Computations* by John Skilling. pp 507–512
- Feroz F., Hobson M. P., Bridges M., 2009, *MNRAS*, 398, 1601
- Hamerly G., Elkan C., 2003, in *Proceedings of the 17-th annual conference on Neural Information Processing Systems (NIPS)* pp 281–288
- Hobbs G., Edwards R., Manchester R., 2006, *Chinese Journal of Astronomy and Astrophysics Supplement*, 6, 020000
- Newman M., Barkema G., 1999, *Monte Carlo Methods in Statistical Physics*. Oxford University Press Inc., pp 31–86
- Newton M. A., Raftery A. E., 1994, *Journal of the Royal Statistical Society, Series B*, 56, 3
- Pelleg D., Moore A., 2000, in *Proceedings of the 17-th International Conference on Machine Learning* pp 727–734
- Roberts G., Gelman A., Gilks W., 1997, *Ann. of Appl. Prob.*, 7, 110
- Skilling J., 2004, in R. Fischer, R. Preuss, & U. V. Toussaint ed., *American Institute of Physics Conference Series Vol. 735 of American Institute of Physics Conference Series, Nested Sampling*. pp 395–405
- van Haasteren R., Levin Y., McDonald P., Lu T., 2009, *MNRAS*, 395, 1005
- Verbiest J. P. W., Bailes M., Coles W. A., Hobbs G. B., van Straten W., Champion D. J., Jenet F. A., Manchester R. N., Bhat N. D. R., Sarkissian J. M., Yardley D., Burke-Spolaor S., Hotan A. W., You X. P., 2009, *ArXiv e-prints*
- Weinberg M. D., 2009, *ArXiv Astrophysics e-prints*